

New Extended Discrete First-Order Model to Reproduce Propagation of Jam Waves

Han, Yu; Yuan, Yufei; Hegyi, Andreas; Hoogendoorn, Serge

DOI

[10.3141/2560-12](https://doi.org/10.3141/2560-12)

Publication date

2016

Document Version

Accepted author manuscript

Published in

Transportation Research Record

Citation (APA)

Han, Y., Yuan, Y., Hegyi, A., & Hoogendoorn, S. (2016). New Extended Discrete First-Order Model to Reproduce Propagation of Jam Waves. *Transportation Research Record*, 2560, 108-118.
<https://doi.org/10.3141/2560-12>

Important note

To cite this publication, please use the final published version (if applicable).
Please check the document version above.

Copyright

Other than for strictly personal use, it is not permitted to download, forward or distribute the text or part of it, without the consent of the author(s) and/or copyright holder(s), unless the work is under an open content license such as Creative Commons.

Takedown policy

Please contact us and provide details if you believe this document breaches copyrights.
We will remove access to the work immediately and investigate your claim.

A new extended discrete first-order model to reproduce the propagation of jam waves

Yu Han

Department of Transport & Planning
Faculty of Civil Engineering and Geosciences, Delft University of Technology
PO Box 5048, 2600 GA Delft – The Netherlands
Phone +31 15 278 46 72 Fax +31 15 278 31 79
e-mail y.han-1@tudelft.nl

Yufei Yuan

Department of Transport & Planning
Faculty of Civil Engineering and Geosciences, Delft University of Technology
PO Box 5048, 2600 GA Delft – The Netherlands
Phone +31 15 278 40 66 Fax +31 15 278 31 79
e-mail y.yuan@tudelft.nl

Andreas Hegyi

Department of Transport & Planning
Faculty of Civil Engineering and Geosciences, Delft University of Technology
PO Box 5048, 2600 GA Delft – The Netherlands
Phone +31 15 278 96 44 Fax +31 15 278 31 79
e-mail a.hegyi@tudelft.nl

Serge P. Hoogendoorn

Department of Transport & Planning
Faculty of Civil Engineering and Geosciences, Delft University of Technology
PO Box 5048, 2600 GA Delft – The Netherlands
Phone +31 15 278 54 75 Fax +31 15 278 31 79
e-mail s.p.hoogendoorn@tudelft.nl

Abstract + Main text: 5741
Figures & Tables: $5 \times 250 = 1250$
26 references=500
Total: $5741 + 1250 + 500 = 7491$

TRR Paper number: 16-3482

Submission Date: 10/03/2016

ABSTRACT

In this paper we propose an extension of the discrete LWR model of the cell-transmission model type, to reproduce the capacity drop and the propagation of jam waves. Recently studies have tried to incorporate the capacity drop into discrete first-order traffic flow models for traffic optimization purpose. It is found that the inflow to a discharging cell predicted by these models might have been overestimated, which will influence the propagation of a jam wave. Empirical analysis has been carried out to confirm this assumption. Furthermore, it is found that the extent of the flow reduction depends on the state difference between the targeting cell and its upstream cell. Based on these findings, a new mathematical model formulation is given. Simulations with both a hypothetical freeway stretch and a real life freeway stretch are performed to test the behaviour of the proposed model. The previously mentioned models are also simulated for comparison. Simulation results indicate that the proposed model has a better performance in reproducing jam waves. In addition, the proposed model can be used in a linear model predictive control framework, and formulated as a linear optimization problem, which may be beneficial for a real-life, real-time application.

Keywords: first-order traffic flow model, jam wave, capacity drop.

1 INTRODUCTION

Traffic flow models play an important role in evaluating the impact of traffic congestion and developing efficient traffic control strategies for traffic networks. In the last decades, several freeway traffic flow models have been presented for both simulation and control purposes. Dynamic freeway traffic flow modelling started from (1-2), which developed the first dynamic traffic flow model (LWR model), based on a hyperbolic partial differential equation. The LWR model mainly contains two equations, one is the vehicle conservation equation, and the other one is known as the fundamental diagram. Based on this representation, Daganzo (3) proposed a discretized version of the LWR model, known as the cell-transmission model. Afterwards, many variants of the discrete first-order model have been presented in (4-7).

The cell-transmission model and many of its variants are solved by a minimum demand (sending capacity) and supply (receiving capacity) method, based on the Eulerian (space-time) formulation (8), for calculating the fluxes at discrete cell boundary. By knowing the current state of the cells and parameters of the fundamental diagram, the fluxes between cells can be calculated, and the cell state can be predicted over time. One advantage of these models is that they can easily be deployed to solve a linear optimization problem for traffic control. The maximization of the network throughput can be represented by a linear function of fluxes between cells. The fluxes that are determined by the minimum of the demand and the supply functions, can be represented by linear inequality constraints. Therefore, the optimal control scheme can be determined by solving a linear programming problem. For example, Ziliaskopoulos (25) applied the cell-transmission model for network optimization based on a linear programming problem. Gomes and Horowitz (4) developed a linear model predictive control strategy based on an asymmetric cell transmission model.

For the purpose of developing efficient control strategies, it is important that discrete first-order models can reproduce the relevant traffic phenomena, such as the propagation of shockwaves and spillbacks. However, there are still many traffic phenomena that a discrete first-order model could not reproduce, such as jam waves, traffic oscillations, and traffic hysteresis.

Different higher-order models have been developed to overcome the shortcomings of first-order models. For a review of different models readers can refer to (9). In higher-order models, such as METANET (10), the propagation of a jam wave can be reproduced by describing the spatial temporal evolution of speed. An important drawback of high-order model is that drivers may be affected by the traffic condition behind them (11). This criticism has been addressed by the ARZ model (26), which has the anisotropic property. But still, due to the non-linearity of high-order traffic flow models, the optimization problems based on this kind of models are often difficult to be solved efficiently and accurately.

In short, a well-developed traffic flow model should have a good trade-off in reproducing congestion levels, understanding traffic phenomena, and developing efficient control strategies. Previous freeway traffic flow models in literatures have some shortcomings, either in describing traffic phenomena or in developing efficient control strategies. At the moment, a freeway traffic flow model that can reproduce relevant traffic characteristics for control and that can be efficiently solved is still lacking.

In general, two types of traffic jams on freeways can be identified. As has been presented in (12), traffic jams with the head fixed at the bottleneck are known as standing queues, and jams that have an upstream moving head and tail are known as jam waves (also known as wide

moving jam in some studies, e.g. (15)). A standing queue can be formed at a busy on-ramp, a lane drop bottleneck, or any kind of infrastructural bottlenecks. It can be reproduced by many discrete first-order models, as will be shown in section 4 of this paper. A jam wave generates various negative effects. For example, it reduces freeway capacity, triggers standing queue, and results in travel delays and unsafe traffic conditions. Therefore, it is important for a traffic flow model to reproduce jam waves. As we know, the formation of a jam wave is stochastic and not easy to predict (17). By Laval and Leclercq a possible explanation is provided for the spontaneous appearance of stop-and-go waves as a result of very small disturbances (23). However their explanation is in terms of a microscopic car-following model, and it is not trivial to translate it into a macroscopic (and linear) description. For these reasons, we will focus on the reproduction of jam wave propagation after it has occurred, which follows known patterns.

The outflow of a jam wave is lower than the free flow capacity, as a result of the capacity drop phenomenon. Recently, some studies have tried to incorporate the capacity drop into first-order traffic flow models. Leclercq et al. (24) proposed an analytical model to predict the capacity drop at an active merge bottleneck. Schreiter et al. (13) assumed two constant capacity values for the cell-transmission model, one for free flow condition and the other for congested condition. Srivastava and Geroliminis (14) also proposed an extended LWR model with two capacity values, and they provided a memory-based methodology to choose the appropriate value of capacity for the numerical solution. The research shed light on different ways of modelling the capacity drop. However due to the non-linearity, these models have not been utilized for traffic control.

Some discrete first-order models which incorporated with the capacity drop, have been developed into traffic optimizations. Muralidharan (5) incorporated the capacity drop into a link-node cell-transmission model, which uses a discontinuous fundamental diagram. The capacity drop was assumed to be triggered on only at the bottleneck cell, with a constant value. Roncoli et al. (6) proposed an optimization-oriented first-order model, which also represented the capacity drop by a reduced demand function. They assumed that the extent of the demand reduction of a cell has a linear relation with the vehicle density of the same cell. In our previous work, a similar assumption has been made (7). We also assumed that the extent of the capacity drop of a cell has a linear relation, but with the density of the upstream cell. In this way the capacity drop at lane-drop bottleneck can also be reproduced. These model have been proposed for traffic optimizations, however, none of them have been validated in reproducing the propagation of jam waves.

The main contribution of this paper is that we compare the performance of different discrete first-order models that can be used in an optimization framework (i.e. can be formulated as a linear QP problem) in reproducing jam waves. After analyzing the shortcomings of these models, a new discrete first-order model is developed and validated. Besides the ability in reproducing the propagation of jam waves, the proposed model keeps the linear property of previous ones, which makes it applicable into a linear optimization problem for traffic control.

The organizing of the paper is as follows. In Section 2 we practically describe the traffic flow features of the jam wave and theoretically analyze the reason why existing discrete first-order traffic flow models could not reproduce the propagation of a jam wave accurately. It is found that the supply function of the classical discrete first-order models might not be applicable to the moving jam condition. In Section 3, an empirical study is performed to check if the real data matches the theoretical findings. After checking the data, in Section 4, two reasonable assumptions are made. Based on these two assumptions, the detailed mathematical formulation

of the first-order traffic flow model is given. In Section 5, the model is validated by both a synthetic case and a real life case. In the last section, we present the main conclusion and propose the future research direction.

2 DESCRIPTION AND ANALYSIS OF JAM WAVES

2.1 Practical Description

A jam wave is a common traffic flow phenomenon on freeways. It usually originates from a traffic breakdown, which is caused for instance by a vehicle suddenly braking or lane changing in a high-demand traffic flow situation. Therefore, since so many (partially unobservable) factors influence the formation process, the formation of a jam wave is considered stochastic and difficult to be reproduced. From different empirical studies, some common patterns of its propagation can be distilled. For example, the propagation speed of jam waves is relatively stable, typically between 15-20 km/h (16-17). The flow downstream of a jam wave is significantly lower (around 30 percent lower) than the free flow capacity, which is caused by the capacity drop phenomenon (17). It can propagate for a long time period and distance, and resolves only with the traffic demand decreasing (15). In order to illustrate these features, we consider the time-space contour plots of a moving jam on the A13 freeway in the Netherlands that took place on 04-Sep-2012. As shown in Fig. 1 (a), the speed reduction started at detector 4 and propagated to detector 16. It propagated for about 5 km and lasted for about 15 minutes, meaning that the propagation speed is around 20km/h. The reason why the jam is resolved might be attributed to the decreased demand upstream of the jam, as shown in the dashed rectangle area in Fig. 1 (b). It can be found that the capacity drop phenomenon is associated with the jam wave. As shown by the solid triangle area in Fig. 1 (b), the queue discharge rate (green and yellow area, around 6000 veh/h) of the congestion is much less than the free flow capacity (red areas, around 8000 veh/h).

2.2 Theoretical Analysis

The example of the last section shows that the capacity drop associated with a jam wave. In reality the inflow to a jam wave is always slightly lower than the capacity flow, since the critical state is not stable. The outflow of a jam will be higher than the inflow if the capacity drop is not taken into consideration in a traffic flow model, and the jam will be resolved in propagation. Therefore, incorporating the capacity drop is the requirement for a traffic flow model to reproduce the propagation of jam wave. For example, the density-flow diagram of a freeway stretch is represented by Fig.1 (d). State 2 represents the jam state, and 1 represents the traffic state out of the jam. Thus according to the shock wave theory (1-2), if the inflow to the jam equals the outflow of the jam, the propagation of the jam wave is shown in the time-space graph of Fig. 1 (c).

Recently, some approaches have incorporated the capacity drop into discrete first-order traffic flow models (4-7). These models are the variants of the cell-transmission model, and are solved by the minimum demand and supply method. In addition, they have been used as the underlying models for linear optimization problems, which is consistent with the objective of this paper. For traffic control applications, the freeway networks are always divided into cells with a typical length of several hundred meters, which on one hand guarantees a fast computation and on the other hand, is convenient for traffic state estimations. However, when a cell's length becomes large, its traffic state might be inhomogeneous, which might result in inaccurate flow predictions since the fundamental diagram represents the density-flow relations for homogeneous traffic states (18). For instance, when a cell is in a mixed state with a less congested front part and a more congested back part (we define it as the discharging state), its average density is

lower than the density of the back part. Under this circumstance, the inflow to a discharging cell might be overestimated by the previous models, which will influence the propagation of a jam wave.

For example, the space and time are divided discretely, shown as i , $i + 1$, and t_1 , t_2 in Fig. 1(c). At time step t_2 , cell $i + 1$ is in a discharging state. The boundary flux $q_{i \rightarrow i+1}$ is determined based on the average density of cell $i + 1$, because the receiving capacity is dominant in determining the flux. However, since the back part of cell $i + 1$ is more congested than the front part, calculating the flux based on an average density might overestimate the flux, and this will influence the jam wave propagation since the congestion accumulation of cell i is slowing down. We further investigate this assumption through empirical analysis and simulations in the next sections.

3 MODEL DEVELOPMENT

3.1 Empirical Analysis

To understand the key mechanism that a discrete first-order model requires to capture to be able to correctly reproduce jam waves, empirical analysis has been performed. The site we choose is part of British motorway M42 (21). We have chosen this site since there are enough detectors on a homogeneous freeway stretch, which can provide sufficient data for analysis. As shown in Fig. 2 (a), there are nine detectors (8-16) placed every one hundred meters on the homogeneous freeway stretch with same geometric structure. The detectors recorded the speed and detected time of every single vehicle, so we can calculate the harmonic mean speed to approximate the space mean speed, which is more accurate than the time mean speed often provided by other databases.

Data were obtained on day 03-Oct-2008, between 12:00 to 18:00 for the analysis. In this period, both the free flow state, a state close to capacity, and congestion state can be found. Additionally, several moving jams have formed in this time period, as shown in Fig. 2 (b). To see if the supply function of the cell-transmission model is applicable for a discharging cell, we should compare the supply of a receiving cell between when it is in discharging state with when it is not. The following shows the process of selecting appropriate data for analysis.

Assume that the freeway stretch is divided into cells by the detectors, and that we let the detectors represent the downstream boundary of cells. For cells 8-16, the sending cell is represented by i , and the receiving cell is represented by $i + 1$. If cell $i + 1$ is in discharging state, the following conditions should be satisfied.

$$\begin{cases} \rho_{i+1} \geq \rho_{cr} & (a) \\ \rho_i > \rho_{i+1} + \delta_1 > \rho_{i+2} + \delta_2, \delta_1 \geq \delta_2 > 0 & (b) \\ v_i < v_{i+1} + \xi_1 < v_{i+2} + \xi_2, 0 < \xi_1 \leq \xi_2 & (c) \end{cases} \quad (1)$$

For the cell-transmission model, the supply function of a receiving cell is dominant in determining the flux when the density of the receiving cell is beyond the critical value. Thus, the first requirement is that the density of cell $i + 1$ is higher than the critical density, formulated as condition (1a). To determine the value of the critical density, the flow-density plot (fundamental diagram) of the freeway stretch is plotted, and shown in Fig. 2 (c). From the figure we can see that the critical density is higher than 100 veh/km. To make sure all the selected states are in congested condition, we only collected the data that $\rho_{i+1} \geq 120$. Note that for British motorway M42, speed limit control is activated when jam wave occurred, with the value 40 or 50 mph typically. This causes a kind of double structure (two free flow branches) of the fundamental diagram shown in Fig. 2 (c). The speed limit will not have any influence on our analysis, because

we only collect data for congestion condition.

Since a jam wave propagates from the downstream to the upstream cell, if cell $i + 1$ is in discharging state, then cell $i + 2$ should be in the discharging state or free flowing state, and cell i should be in the congestion accumulating state. Thus, the density of cell $i + 1$ should be higher than that of cell i , and lower than the density of cell $i + 2$, shown as (1b). The speed of cell $i + 1$ should be higher than that of cell $i + 2$, and lower than the density of cell i , shown as (1c). δ , ξ are adjustable parameters which are relevant to the width of the moving jam. δ_1 and δ_2 are set to 10, ξ_1 and ξ_2 are set to 3 in this case, based on an experiential test.

If all conditions in (1) are satisfied, the points $(\rho_{i+1}, q_{i \rightarrow i+1})$ are plotted on the left picture of Fig. 2 (d), which are highlighted as red circles. $q_{i \rightarrow i+1}$ is the boundary flux from cell i to cell $i + 1$. If cell $i + 1$ is not in discharging state, the following requirements should be satisfied.

$$\begin{cases} \rho_{i+1} \geq \rho_{cr} & (a) \\ \rho_i < \rho_{i+1} < \rho_{i+2} & (b) \\ v_i > v_{i+1} > v_{i+2} & (c) \end{cases} \quad (2)$$

If the above conditions are satisfied, the points $(\rho_{i+1}, q_{i \rightarrow i+1})$ are plotted on the left picture of Fig. 2 (d), which are highlighted as red stars. The red star scatters are linearly fitted, as shown in the figure, and can be perceived as the congestion branch of a fundamental diagram. The result clearly shows that for a same density value, the flux $q_{i \rightarrow i+1}$ which under conditions in (1), are lower than those under conditions in (2). We will refer to this phenomenon as the supply drop.

The influence of the extent of supply drop is also investigated. We recall the capacity drop assumption made in our previous work. The extent of the capacity drop for a free flowing cell depends on the density difference between this cell and the upstream cell. This inspires us to make a similar assumption that the supply drop level also depends on the density difference between two consecutive cells.

To investigate this assumption, the red circles in the left picture of Fig. 2 (d) are divided into two groups. If $\rho_i - \rho_{i+1} \geq 30$, points $(\rho_{i+1}, q_{i \rightarrow i+1})$ are plotted as blue circles. If $10 < \rho_i - \rho_{i+1} < 30$, points $(\rho_{i+1}, q_{i \rightarrow i+1})$ are still represented by red circles, which are shown in the right picture of Fig. 2 (d). It is obvious that the value of $q_{i \rightarrow i+1}$ are lower when $10 < \rho_i - \rho_{i+1} < 30$ than when $\rho_i - \rho_{i+1} \geq 30$. Therefore, from the analysis of this case, it can be observed that the extent of the supply drop has a positive relation with the density difference between the sending cell and the receiving cell.

3.2 A New Discrete First-order Model

The model development process is divided into 4 steps. At step 1, the new supply function of a discharging cell is introduced with a homogeneous freeway stretch. Based on the new supply function, the equations in determining the flux between cells are proposed at step 2. Step 3 extends the proposed model from homogeneous freeway stretches to generic situations. Step 4 elaborates the node models for merging and diverging, so that the proposed model can be applied to a network.

Step 1. Two reasonable assumptions are made in the last sub-section. a). The existence of the supply drop. Under the same density condition, the supply of a discharging cell is lower than a non-discharging cell. b). The extent of the supply drop has a positive relation with the density difference between the sending cell and the receiving cell. Based on these two assumptions, a new supply function is proposed,

$$\begin{cases} S_{i+1}^{(1)} = \beta_{i+1}^{(1)}(\rho_{i+1}^J - \rho_{i+1}), \rho_i \leq \rho_{i+1} & (a) \\ S_{i+1}^{(2)} = a + b(\rho_i - \rho_{i+1}), \rho_i \geq \rho_{i+1} & (b) \end{cases} \quad (3)$$

where, $S_{i+1}^{(1)}$ is the supply of cell $i + 1$ when it is in non-discharging state, which is represented by $\rho_i \leq \rho_{i+1}$. $S_{i+1}^{(2)}$ is the supply cell $i + 1$ when it is in discharging state, represented by $\rho_i \geq \rho_{i+1}$. $\beta_{i+1}^{(1)}$ is the congestion wave speed of the cell-transmission model, as indicated from Fig. 3 (a). ρ_{i+1}^J is the jam density of cell $i + 1$. The supply of a discharging cell is assumed to have a linear relationship with the density difference between the sending cell and the receiving cell, so coefficient a and b are constant. If $\rho_i = \rho_{i+1}$, based on (3a), $S_{i+1}^{(2)} = a$, and based on (3b), $S_{i+1}^{(1)} = \beta_{i+1}^{(1)}(\rho_{i+1}^J - \rho_{i+1})$. When $\rho_i = \rho_{i+1}$, $S_{i+1}^{(1)} = S_{i+1}^{(2)}$. Thus, $a = \beta_{i+1}^{(1)}(\rho_{i+1}^J - \rho_{i+1})$. For homogeneous cells, $\rho_i^J = \rho_{i+1}^J$. Thus, $a = \beta_{i+1}^{(1)}(\rho_i^J - \rho_i)$.

If $\rho_i > \rho_{i+1}$, and $\rho_{i+1} = \rho_{i+1}^{cr}$, the capacity drop phenomenon happens because the receiving cell is in the free flowing state. According to our previous assumptions, the queue discharge rate of cell $i + 1$, c'_{i+1} is,

$$c'_{i+1} = c_{i+1} \left(1 - \alpha_{i+1} \frac{\rho_i - \rho_i^{cr}}{\rho_i^J - \rho_i^{cr}}\right) \quad (4)$$

where, α_{i+1} is the maximum extent of the capacity drop of cell $i + 1$. ρ_i^{cr} is the critical density of cell i .

In (4), if $\rho_i = \rho_i^J$, then $c'_{i+1} = c_{i+1}(1 - \alpha_{i+1})$. In (3a), if $\rho_{i+1} = \rho_{i+1}^{cr} = \frac{c_{i+1}(1 - \alpha_{i+1})}{v_{i+1}}$, (v_{i+1} is the free flow speed of cell $i + 1$), and $\rho_i = \rho_i^J$, then $S_{i+1}^{(2)} = c_{i+1}(1 - \alpha_{i+1})$. Thus, $b = \frac{c_{i+1}(1 - \alpha_{i+1})}{\rho_{i+1}^J - \rho_{i+1}^{cr}}$. b is denoted as $\beta_{i+1}^{(2)}$. It represents the congestion wave speed of a cell when it is in discharging state, as indicated in Fig. 3 (a). Therefore, equation (3b) can be reformulated as,

$$S_{i+1}^{(2)} = \beta_{i+1}^{(1)}(\rho_i^J - \rho_i) + \frac{c_{i+1}(1 - \alpha_{i+1})}{\rho_{i+1}^J - \rho_{i+1}^{cr}} \cdot (\rho_i - \rho_{i+1}) \quad (5)$$

Step 2. Step 1 gives two supply functions of a receiving cell for over-critical condition. For free flow condition, the supply of a receiving cell equals to the queue discharge rate. To summarize, the supply of the receiving cell S_{i+1} , is determined by the following equation,

$$S_{i+1} = \min(S_{i+1}^{(1)}, S_{i+1}^{(2)}, c'_{i+1}) \quad (6)$$

The demand of cell i is determined by the minimum between the actual vehicle demand of this cell and the queue discharge rate of this cell.

$$D_i = \min(\rho_i \cdot v_i, c'_i) \quad (7)$$

where, v_i is the free flow speed of cell i .

The same as the cell-transmission model, $q_{i \rightarrow i+1}$ is determined by the minimum value between D_i and S_{i+1} ,

$$q_{i \rightarrow i+1} = \min(D_i, S_{i+1}) \quad (8)$$

To illustrate the approach, the demand and supply function can be represented by Fig. 3 (a). The demand function is represented by the blue line, and the supply function is represented by the red line. The physical meaning of the proposed model can be explained in this way: suppose that two consecutive cells, cell i and cell $i + 1$ are in jam state at time t_0 . The acceleration process of cell $i + 1$ can be represented by the blue line of the right picture of Fig. 3 (c), while the state change of cell i can be represented by the red line.

Step 3. The proposed model is introduced with a homogeneous freeway stretch. It can be

extended to generic situations. If two consecutive cells have different geometric structure and different fundamental diagrams, for example, with the on-ramp or lane drop in between, then the supply of the receiving cell depends on the mapped state difference. For example, as shown in the Fig. 3 (b), the black lines denote the fundamental diagram of sending cell i , and the solid red lines denote the fundamental diagram of receiving cell $i + 1$. To get the state difference, first we need to map the state of cell i to cell $i + 1$. The mapped state is represented by ρ'_i as shown in Fig. 3 (b). It can be calculated by the following equation,

$$\rho'_i = \frac{c'_{i+1} + \beta_{i+1}^{(2)} \rho_{i+1}^{cr'} - \beta_{i+1}^{(1)} \rho'_{i+1}}{\beta_{i+1}^{(2)} - \beta_{i+1}^{(1)}} \quad (9)$$

Replace ρ_i with ρ'_i in (5), $S_{i+1}^{(2)}$ can be calculated correspondingly.

Step 4. For the proposed discrete models, the state of each cell is updated every time step, by the following equation,

$$\rho_i(k+1) = \rho_i(k) + \frac{T}{L_i} [(q_{i-1 \rightarrow i}(k) - s_i(k) + r_i(k))] \quad (10)$$

where, $\rho_i(k)$ is the density of cell i at time step k . T is the time duration of one time step, L_i is the length of cell i . $s_i(k)$ is outflow of cell i towards the off-ramp. $r_i(k)$ is the inflow to cell i from the on-ramp. $r_i(k)$ is determined by the following equation,

$$r_i(k) = \min\left(\frac{\omega_i(k)}{T}, u_i, \max\left(\frac{u_i}{c_{i-1} + u_i} \cdot S_i(k), S_i(k) - \frac{\rho_i(k) \cdot L_i(k)}{T}\right)\right) \quad (11)$$

where, $\omega_i(k)$ is the vehicle number of on-ramp i . u_i is the saturation flow of on-ramp i . On-ramp flux $r_i(k)$ shares the supply $S_{i+1}(k)$ with the mainstream flux $q_{i \rightarrow i+1}(k)$ proportionally to the capacity or saturation flow, if there are enough demand from both the mainstream and the on-ramp. If the demand from the mainstream is not enough to share the supply, the remaining supply will be distributed to the mainstream flow, and vice versa. $\omega_i(k)$ evolves as the following equation:

$$\omega_i(k+1) = \omega_i(k) + T(d_i(k) - r_i(k)) \quad (12)$$

where, $d_i(k)$ is the demand of on-ramp i at time step k .

Since the model is solved by the minimum value between the demand function and the supply function, and both the demand function and the supply function are piecewise linear, the proposed model can be formulated as a linear optimization problem for traffic control. A referential example can be found in (7).

From the data analysis we know that even though the supply of a cell and the state difference between the targeting cell and the downstream cell have positive relation, their relation is much complex than a linear relation. We assumed a linear relation just for the convenience of future optimizations. However, we believe that the linear relation is sufficient for the proposed model to reproduce the propagation of a jam wave satisfactorily. Specific model validations are performed in the next section.

4 MODEL VALIDATION

To confirm that the proposed model is able to reproduce the propagation of a jam wave satisfactorily, simulations of both a synthetic freeway stretch and a real life freeway stretch are performed. Some of the previous mentioned discrete first-order traffic flow models are also simulated for comparison. The first one is the model from Roncoli et al. (6) (short as model R). The second one is the model from Muralidharan & Horowitz (5) (short as model M). These models are all the variants of the cell transmission model, and they have been used as the underlying models for a linear optimization problems (19-20), which is consistent with the

objective of this work.

4.1 Simulation Test for a Synthetic Freeway Stretch

A hypothetical homogeneous freeway stretch is proposed to test the performance of the proposed models. The two-lanes freeway stretch, is divided into 17 cells of, equal length of 0.6 km, as shown in Fig. 4 (a). The free flow speed is set to 108 km/h, and the capacity is set to 2000 veh/h/lane, so the critical density can be calculated as the division of the capacity and the free flow speed. The wave speed is set to 18 km/h, so the jam density can be known correspondingly. The maximum extent of capacity drop is set to 35% for model R and the proposed model, based on empirical findings (22). The constant capacity drop of model M is set to 15% (19).

The demand profile of the simulation is shown in Fig. 4 (b). Demand decreases from 3800veh/h to 3000 veh/h at time step 280, to show the influence of demand decreasing to the propagation of jam waves. At time step 180, the density of cell 16 is manually set to the jam density, 250veh/km. Then the congestion propagation of the previous mentioned models are simulated. The simulation results are shown in Fig. 4(c-j).

As shown in the density contour plot of Fig. 4, the cell-transmission model and model R show similar results. The jams are resolved, before the traffic demand decreasing. For model M, the jam evolves into a standing queue, because a constant amount of the capacity drop is assumed. The proposed model also shows dispersion, but it is much less than the other models. Before the traffic demand decreasing, traffic jam still exist and is wider than the start. Thus, the proposed model works better in reproducing jam wave in this hypothetical freeway stretch.

The flow contour plots indicate how the capacity drop is reproduced by these models. For the cell-transmission model, the capacity drop is not taken into account, so the outflow from congestion is always the free flow capacity. For model M, the capacity drop only takes place at cell 16. When cell 16 has an equal inflow and outflow, its density stays constant. That is why the congestion head does not move upstream. For model R, even though the capacity drop is assumed to happen for every cell, we can see from fig. 4 (h) that the capacity drop actually only happens at cell 16. The proposed model, by contrast, reproduces the capacity drop better. From fig. 4 (j) it can be seen that the outflow of every cell in jam is less than the free flow capacity.

We have also investigated the models' behaviour as the temporal step tends to zero. The simulation results are similar to the above case, that the dispersion of previous models are conspicuous while the proposed model is much less.

4.2 Simulation tests for a real life freeway stretch

The traffic flow model proposed in the last section is now applied to a particular freeway stretch for model validation. The chosen site is a stretch of Dutch freeway A13, connecting the city Rotterdam and the city Delft. We choose this site because there are not many on-ramps and off-ramps attached to this stretch. In the Netherlands, flows of the on-ramps and the off-ramps are hardly detected. Therefore, the demand of the on-ramp and the splitting ratio of the off-ramp are roughly estimated by the flow difference between the upstream detector and downstream detector of the on-ramp or the off-ramp. If there are too many ramps involved, the estimation errors might be magnified and leads to inaccurate predictions.

The considered stretch has a length of 7.8 km. A graphical representation of the freeway stretch is shown in Fig. 5 (a). There are 19 detectors included in the targeting stretch, which are represented by black dots. Each segment in the figure represents a cell, with a length of 150 m. On-ramps (represented by R1, R2), off-ramps (represented by S1, S2, S3), and lane drop (represented by a red line), divide the freeway stretch into 7 sections. The calibrated capacity (veh/h) of each section are also shown in Fig. 5 (a). Other parameters are assumed to be

constant for all seven sections for convenience. The free flow speed v is set to 108 km/h, the wave speed β_1 is set to 19.5 km/h, the maximum extent of the capacity drop α is set to 35%.

On the day 08-Oct-2012, a jam wave occurred on A13 during the morning peak. The jam was formed at a bottleneck downstream of the targeting stretch and propagated through it. The speed contour plot of the targeting stretch, from 7:30 to 9:30, is shown in Fig. 5 (e). In the simulation, the formation of the jam wave is reproduced by changing the boundary condition. The outflow of the downstream boundary of the freeway stretch is changed to 2000 veh/h manually at time period 8:22-8:25.

Demand profiles of the mainstream and on-ramps are shown in Fig. 5 (b) and (c). Since there are not many vehicles using on-ramp R2, the demand of on-ramp 2 is assumed to be a constant value. The total demand of the considered time period is calculated by the difference between the flow aggregation of the upstream detector and the downstream detector. Figure. 5 (d) is the splitting ratio of three off-ramps. The same as on-ramp 2, off-ramp S2 is also not busy. Thus, the off-ramp splitting ratio of S2 is assumed to be constant as well.

Speed contour plots of the simulations are shown in Fig. 5 (f-i). The cell-transmission model and model R show similar result, that the jam wave does not propagate for a sufficient long time and distance, and it is resolved spontaneously when propagates upstream. For model M, the head of the congestion forms to a standing queue again. Only the proposed model reproduces a satisfactory result that the moving jam propagates through the freeway stretch, which is in line with reality. Note that the proposed model is sensitive to the demand and the value of α . Therefore, the small dispersion shown in the downstream end of Fig. 5 (f) might be attribute to the small detecting error of the demand.

The simulation results are also tested quantitatively. The Root-mean-square error (RMSE) is chosen as the quantitative criteria for evaluating the simulation results. In this case only the time period from 8:22 to 8:53, when the jam wave was taken place at the stretch is selected for calculation. The RMSE is calculated based on the following equation. The RMSE of the proposed model, model R, CTM and model M are 26.98, 34.77, 34.86, and 41.8. Thus, quantitative results also show that the proposed model have a better performance in reproducing jam waves.

$$\text{RMSE} = \sqrt{\frac{\sum_{t=52}^{t=83} (\bar{v}_t - v_t)^2}{32}} \quad (13)$$

5 CONCLUSIONS

In this paper we propose a linear discrete first-order traffic flow model that aims to reproduce the propagation of jam waves.

First, theoretical and empirical analyses are performed to confirm that the supply function of the cell-transmission model is not applicable for the jam wave condition. Two assumptions are made based on theoretical and empirical findings. The first one is a new concept, the supply drop, which means that the supply of a cell should be decreased when the cell is in discharging state. The second one is about the extent of the supply drop. It is assumed that the extent depends on the state difference between two neighbouring cells. Based on these two assumptions, a linear supply function of a discharging-stated cell is proposed. After that, the mathematical formulation of the proposed model is elaborated.

Model validation is performed by data from both simulation of a synthetic freeway stretch and a real life freeway stretch. From the synthetic case, it is shown that the proposed model is able to better reproduce the propagation of jam waves and the capacity drop. For the

real life case, qualitatively, it is found the jam wave reproduced by the proposed model propagates longer in time and space than that reproduced by the other models, which fits reality better. Quantitatively, the root-mean-square error of the proposed model is much lower than that of the other models. It could be concluded that the proposed model has a better performance in reproducing the propagation of jam waves.

Besides the advancement in reproducing traffic phenomena, the proposed model keeps the advantage of the cell-transmission-based models in respect of computation efficiency. The linear property of the proposed model makes it suitable for a linear optimization problem for traffic control purpose. This will be the focus of our future research.

ACKNOWLEDGEMENT

The research leading to these results are sponsored by Chinese Scholarship Council.

REFERENCES

- [1] Lighthill, M.J. and G.B. Whitham. On kinematic waves. II. A theory of traffic flow on long crowded roads. in *Proceedings of the Royal Society of London A: Mathematical, Physical and Engineering Sciences*. 1955. The Royal Society.
- [2] Richards, P.I., 1956. Shock waves on the highway. *Operations research* 4(1), 42-51.
- [3] Daganzo, C.F., The cell-transmission model: A dynamic representation of highway traffic consistent with the hydrodynamic theory. *Transportation Research Part B: Methodological*, 1994. 28(4): p. 269-287.
- [4] Gomes, G. and R. Horowitz, Optimal freeway ramp metering using the asymmetric cell-transmission model. *Transportation Research Part C: Emerging Technologies*, 2006. 14(4): p. 244-262.
- [5] Muralidharan, A., G. Dervisoglu, and R. Horowitz. Freeway traffic flow simulation using the link node cell-transmission model. in *American Control Conference, 2009. ACC'09. 2009. IEEE*.
- [6] Roncoli, C., M. Papageorgiou, and I. Papamichail, Traffic flow optimisation in presence of vehicle automation and communication systems—Part I: A first-order multi-lane model for motorway traffic. *Transportation Research Part C: Emerging Technologies*, 2015. 57: p. 241-259.
- [7] Han, Y., et al. Linear quadratic MPC for integrated route guidance and ramp metering. in *Intelligent Transportation System, 2015. ITSC 2015*.
- [8] Lebacque, J.-P. The Godunov scheme and what it means for first-order traffic flow models. in *International symposium on transportation and traffic theory*. 1996.
- [9] van Wageningen-Kessels, F., et al., Genealogy of traffic flow models. *EURO Journal on Transportation and Logistics*, 2014: p. 1-29.
- [10] Messner, A., and Markos Papageorgiou. "METANET: A macroscopic simulation program for motorway networks." *Traffic Engineering & Control* 31.8-9 (1990): 466-470.
- [11] Daganzo, C.F., Requiem for second-order fluid approximations of traffic flow. *Transportation Research Part B: Methodological*, 1995. 29(4): p. 277-286.

- [12]Hegyi, A., et al. SPECIALIST: A dynamic speed limit control algorithm based on shock wave theory. in Intelligent Transportation Systems, 2008. ITSC 2008. 11th International IEEE Conference on. 2008. IEEE.
- [13]Schreiter T, Smit E, Van Lint H, Hoogendoorn S P. The cell-transmission model with capacity drop. 11th TRAIL Congress, 2012.
- [14]Srivastava, A. and N. Geroliminis, Empirical observations of capacity drop in freeway merges with ramp control and integration in a first-order model. *Transportation Research Part C: Emerging Technologies*, 2013. 30: p. 161-177.
- [15]Kerner, B.S. and H. Rehborn, Experimental features and characteristics of traffic jams. *Physical Review E*, 1996. 53(2): p. R1297.
- [16]Schönhof, M. and D. Helbing, Empirical features of congested traffic states and their implications for traffic modeling. *Transportation Science*, 2007. 41(2): p. 135-166.
- [17]Hoogendoorn, S.P., H. Botma, and M. Minderhoud, *Traffic flow theory and simulation*. TU Delft, 2006.
- [18]van Wageningen-Kessels, F. *Multi-class continuum traffic flow models: Analysis and simulation methods*. Diss. TU Delft, Delft University of Technology, 2013.
- [19]Muralidharan, A. and R. Horowitz, *Computationally efficient model predictive control of freeway networks*. *Transportation Research Part C: Emerging Technologies*, 2015.
- [20]Roncoli, C., M. Papageorgiou, and I. Papamichail, *Traffic flow optimisation in presence of vehicle automation and communication systems—Part II: Optimal control for multi-lane motorways*. *Transportation Research Part C: Emerging Technologies*, 2015. 57: p. 260-275.
- [21]Wilson, R.E. From inductance loops to vehicle trajectories. in *Proc. Symp. Fundam. Diagram—75 years*. 2008.
- [22]Yuan K, Knoop V L, Hoogendoorn S P. Capacity Drop: A Relation Between The Speed In Congestion And The Queue Discharge Rate. *Transportation Research Board 94th Annual Meeting*. 2015 (15-4064).
- [23]Laval, J.A. and L. Leclercq, A mechanism to describe the formation and propagation of stop-and-go waves in congested freeway traffic. *Philosophical Transactions of the Royal Society of London A: Mathematical, Physical and Engineering Sciences*, 2010. 368(1928): p. 4519-4541.
- [24]Leclercq, L., J.A. Laval, and N. Chiabaut, Capacity drops at merges: an endogenous model. *Transportation research part B: methodological*, 2011. 45(9): p. 1302-1313.
- [25]Ziliaskopoulos, A.K., A linear programming model for the single destination system optimum dynamic traffic assignment problem. *Transportation science*, 2000. 34(1): p. 37-49.
- [26]Aw A, Rascle M. Resurrection of " second order" models of traffic flow. *SIAM journal on applied mathematics*, 2000, 60(3): 916-938.

LIST OF FIGURES

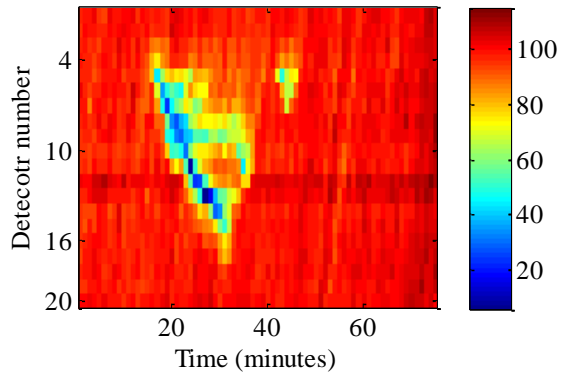
FIGURE 1 Visualization of jam waves from empirical data and theoretical analysis. Empirical data were obtained from loop detectors of Dutch freeway A13. There are four lanes for this freeway stretch.

FIGURE 2 The targeting stretch, and analyzing results of the empirical study.

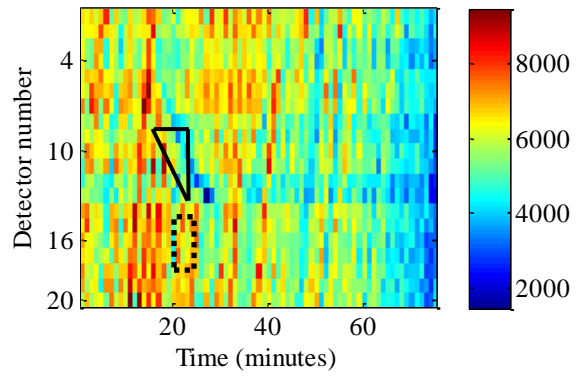
FIGURE 3 Description of the proposed model. (a) shows the demand and the supply function of the proposed model. (b) represents the different fundamental diagram of two consecutive cells. (c) shows the acceleration process of two neighbouring jam cells.

FIGURE 4 The hypothetical freeway stretch, demand profile, and simulation results

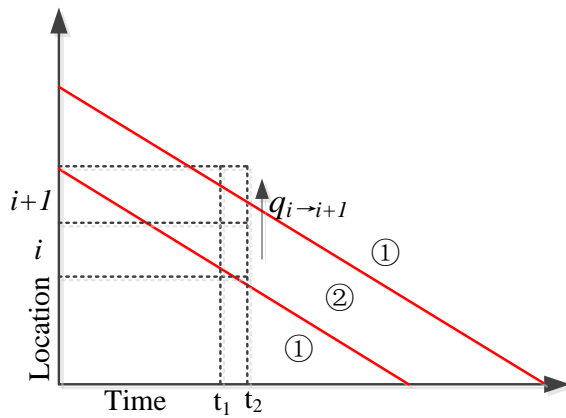
FIGURE 5 The real life freeway stretch, demand profiles, and simulation results.



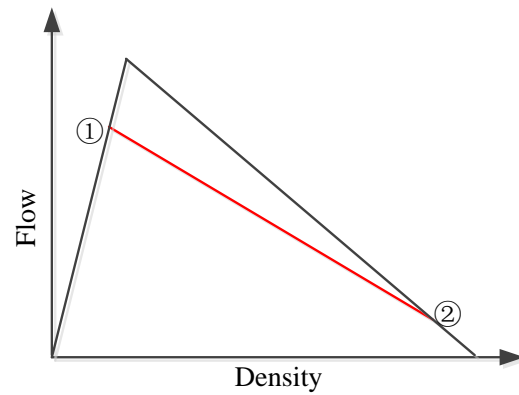
(a) The speed contour plot of a moving jam



(b) The flow contour plot of a moving jam

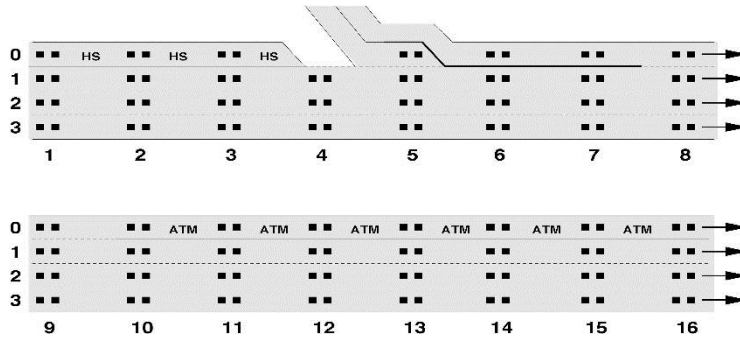


(c) The jam wave propagation

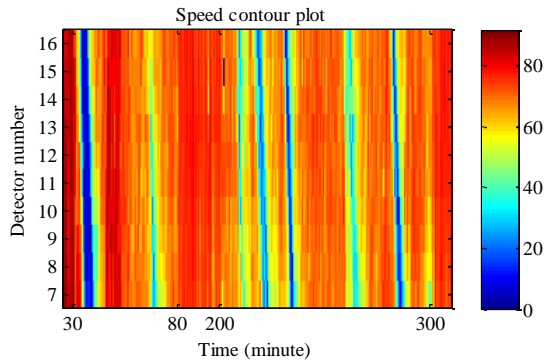


(b) The density-flow diagram

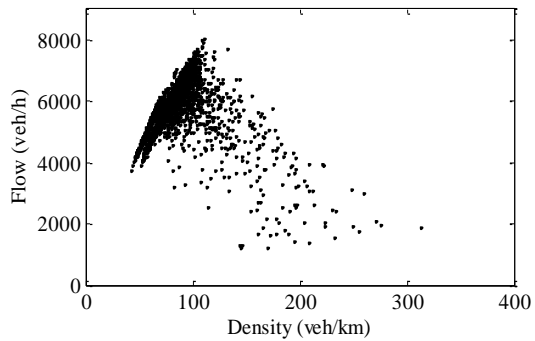
FIGURE 1 Visualization of jam waves from empirical data and theoretical analysis. Empirical data were obtained from loop detectors of Dutch freeway A13. There are four lanes for this freeway stretch.



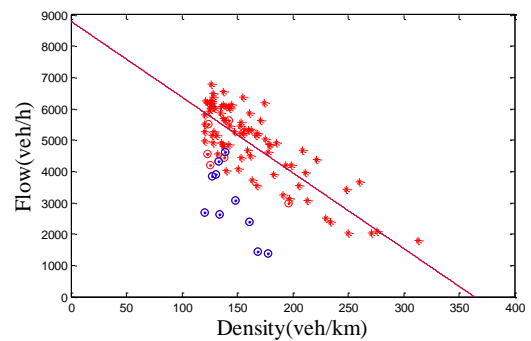
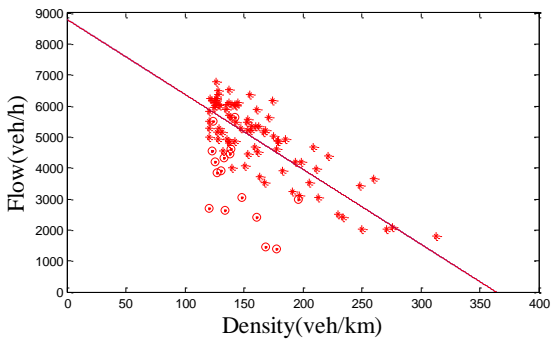
(a) The layout of the targeting stretch of British freeway M42. HS denotes the hard shoulder, and active traffic management (ATM) denotes hard shoulder open for traffic during peak hour.



(b) Speed contour plot of the analyzing period



(c) Fundamental diagram



(d) Data analysis of the proposed site. The plots represent the relation between density ρ_{i+1} and flux $q_{i \rightarrow i+1}$, $8 \leq i < 16$.

FIGURE 2 The targeting stretch, and analyzing results of the empirical study.

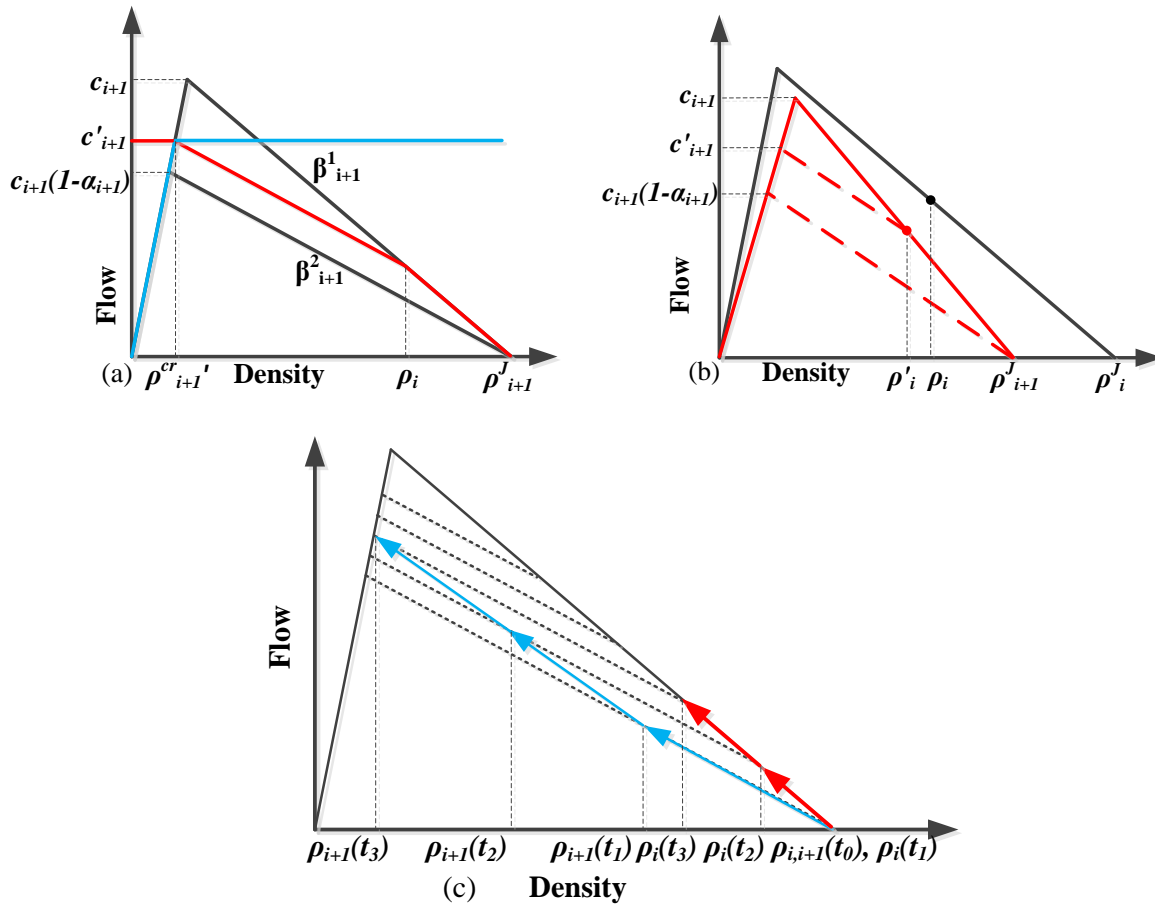
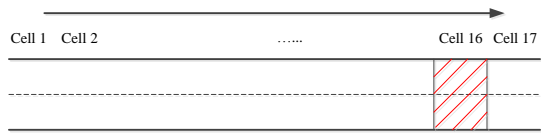
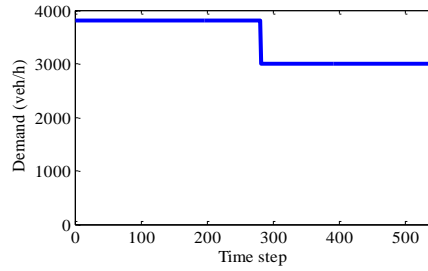


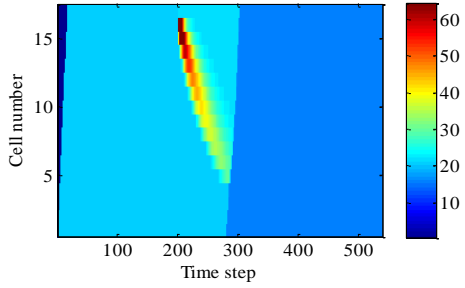
FIGURE 3 Description of the proposed model. (a) shows the demand and the supply function of the proposed model. (b) represents the different fundamental diagram of two consecutive cells. (c) shows the acceleration process of two neighbouring jam cells.



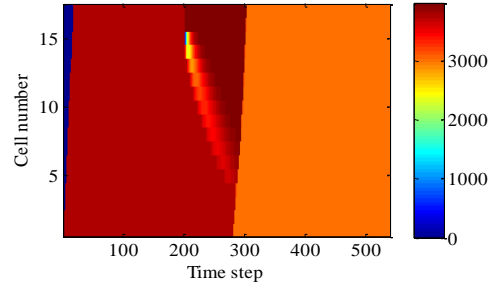
(a) The hypothetical freeway stretch



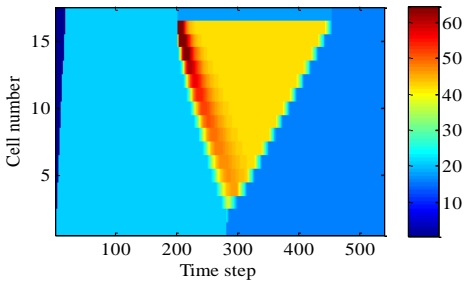
(b) Demand profiles



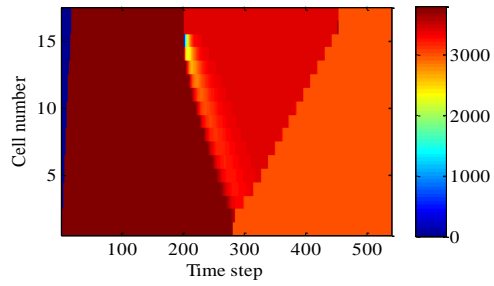
(c) Density contour simulated with CTM



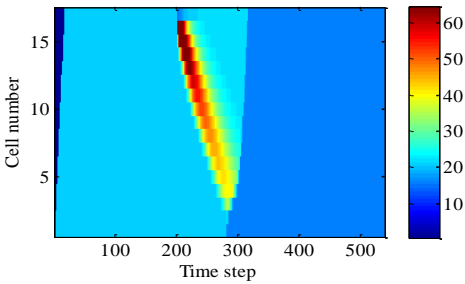
(d) Flow contour simulated with CTM



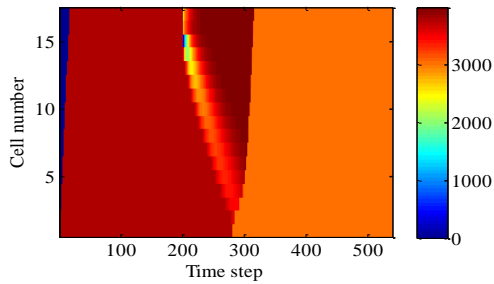
(e) Density contour simulated with model M



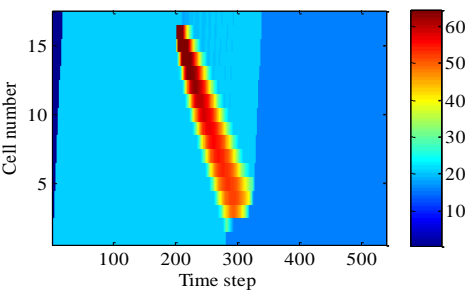
(f) Flow contour simulated with model M



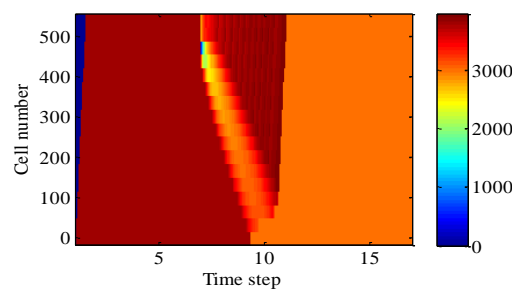
(g) Density contour simulated with model R



(h) Flow contour simulated with model R

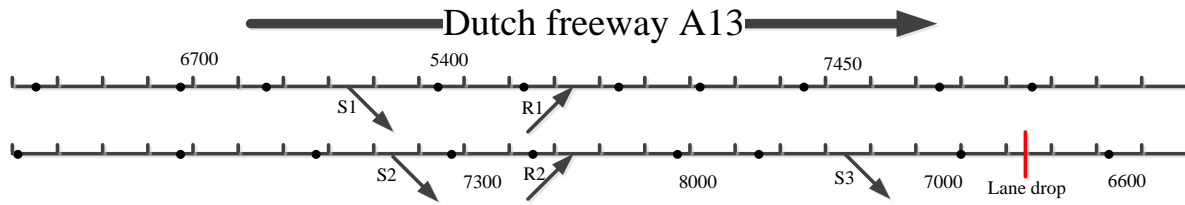


(i) Density contour simulated with the proposed

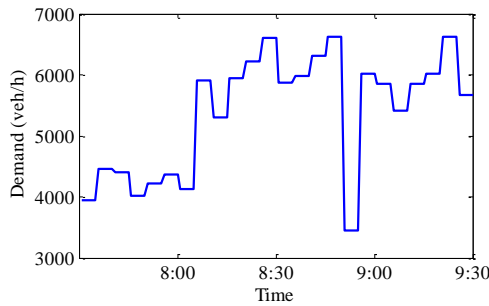


(j) Flow contour simulated with the proposed

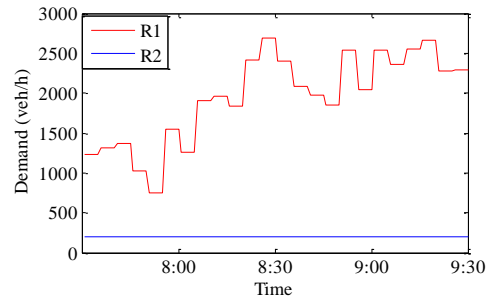
FIGURE 4 The hypothetical freeway stretch, demand profile, and simulation results



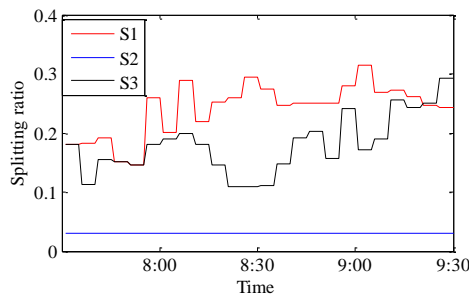
(a) A graphical representation of the freeway stretch



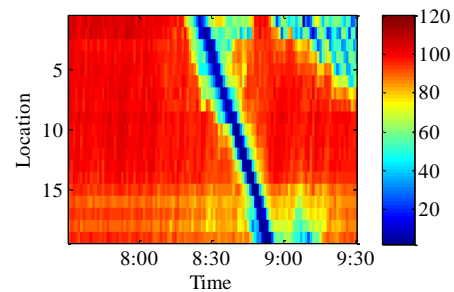
(b) Demand profile of the mainstream



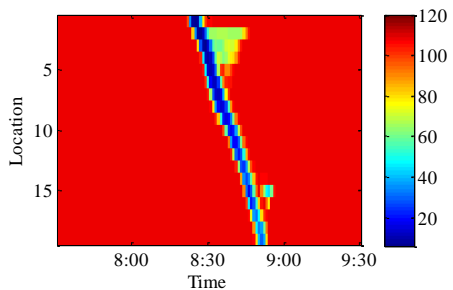
(c) Demand profile of the on-ramps



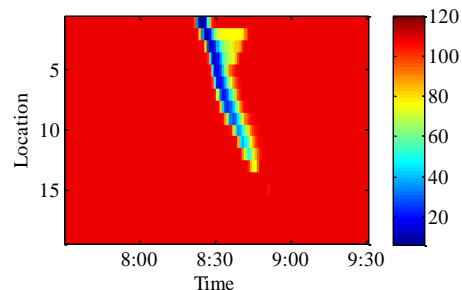
(d) Splitting ratio of off-ramps



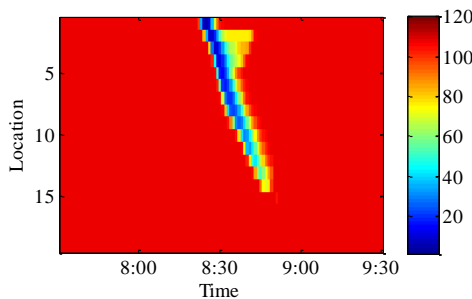
(e) Speed contour plot of real data



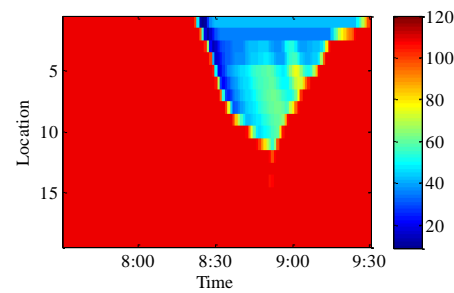
(f) Speed contour plot of the proposed model



(g) Speed contour plot of CTM



(h) Speed contour plot model R



(i) Speed contour plot of model M

FIGURE 5 The real life freeway stretch, demand profiles, and simulation results.